PLOS ONE

Adjuvant chemotherapy or no adjuvant chemotherapy? A prediction model for the risk stratification of recurrence or metastasis of nasopharyngeal carcinoma combining MRI radiomics with clinical factors

Qiaoyuan Wu[1☯], Yonghu Chang[2☯], Cheng Yang[3], Heng Liu[4], Fang Chen[1], Hui Dong[1], Cheng Chen[5]*, Qing Luo[1]*

1 The Public Experimental Center of Medicine, Department of Pathology, Affiliated Hospital of Zunyi Medical University, Zunyi, Guizhou, P. R. China, 2 School of Medical Information Engineering of Zunyi Medical University, Zunyi Medical University, Zunyi, Guizhou, P. R. China, 3 The Third Clinical Medical College of Ningxia Medical University, Yinchuan, Ningxia, P. R. China, 4 Department of Radiology, Affiliated Hospital of Zunyi Medical University, Zunyi, Guizhou, P. R. China, 5 Department of Thoracic Surgery, Affiliated Hospital of Zunyi Medical University, Zunyi, Guizhou, P.R. China

☯ These authors contributed equally to this work.
* zlsysluoqing@163.com (QL); 29217036@qq.com (CC)

OPEN ACCESS

Abstract

Background

Dose adjuvant chemotherapy (AC) should be offered in nasopharyngeal carcinoma (NPC) patients? Different guidelines provided the different recommendations.

Methods

In this retrospective study, a total of 140 patients were enrolled and followed for 3 years, with 24 clinical features being collected. The imaging features on the enhanced-MRI sequence were extracted by using PyRadiomics platform. The pearson correlation coefficient and the random forest was used to filter the features associated with recurrence or metastasis. A clinical-radiomics model (CRM) was constructed by the Cox multivariable analysis in training cohort, and was validated in validation cohort. All patients were divided into high- and low-risk groups through the median Rad-score of the model. The Kaplan-Meier survival curves were used to compare the 3-year recurrence or metastasis free rate (RMFR) of patients with or without AC in high- and low-groups.

Results

In total, 960 imaging features were extracted. A CRM was constructed from nine features (seven imaging features and two clinical factors). In the training cohort, the area under curve (AUC) of CRM for 3-year RMFR was 0.872 (P <0.001), and the sensitivity and specificity were 0.935 and 0.672, respectively; In the validation cohort, the AUC was 0.864 (P <0.001), and the sensitivity and specificity were 1.00 and 0.75, respectively. Kaplan-Meier curve

showed that the 3-year RMFR and 3-year cancer specific survival (CSS) rate in the high-risk group were significantly lower than those in the low-risk group (P <0.001). In the high-risk group, patients who received AC had greater 3-year RMFR than those who did not receive AC (78.6% vs. 48.1%) (p = 0.03).

Conclusion

Considering increasing RMFR, a prediction model for NPC based on two clinical factors and seven imaging features suggested the AC needs to be added to patients in the high-risk group and not in the low-risk group.

1. Introduction

Nasopharyngeal carcinoma (NPC) is a malignant tumour of the head and neck originating from the nasopharyngeal mucosal lining with uneven endemic distribution [1]. According to the 2020 Global Cancer Statistics, the new incidence and new mortality of NPC accounted for 0.7% and 0.8% of all cancers, respectively [2].

At present, tumour node-metastasis (TNM) stage is one of the most important factors in predicting the prognosis of NPC. However, the prognosis of patients with the same TNM stage receiving similar treatment varies greatly. 20%-30% patients still experienced recurrence or metastasis, resulting in poor prognosis [3, 4]. This phenomenon may be explained by this fact that the TNM staging system mainly reflects the degree of invasion of the tumour anatomical structure and cannot accurately reflect the heterogeneity within the tumour.

Adjuvant chemotherapy (AC) refers to chemotherapy performed after radical local treatment (surgery or radiotherapy) to prevent the recurrence or metastasis of micrometastatic lesions that may exist. Chen et al. found that AC did not improve failure-free survival after concurrent chemoradiotherapy (CCRT) in locoregionally advanced nasopharyngeal carcinoma (LA-NPC) [5]. Therefore, for patients with LA-NPC, CSCO recommends induction chemotherapy (IC) combined with concurrent radiotherapy (CCRT) as category IA and CCRT combined with AC as category IB [6]. However, The National Comprehensive Cancer Network (NCCN) and European Society for Medical Oncology (ESMO) guidelines recommend that IC and AC have equal status [7, 8]. Does AC benefit patients? In order to solve the problem, many scholars stratified NPC patients and found that AC was suitable for some specific populations and improved survival, such as N stage stratification, EB virus infection stratification [9–12]. Therefore, A more accurate combined model is necessary to predict the prognosis of NPC and identify patients who may benefit from AC.

Radiomics refers to the extraction and analysis of a large number of advanced quantitative imaging features from medical images [13, 14]. As a new technique, radiomics has been studied for many applications, such as clinical diagnostics, pathological typing, prognosis prediction and clinical decision-making for a variety of cancers, including lung cancer, colon cancer and kidney cancer [15–18]. In many studies, radiomics demonstrated a good predictive ability [19, 20], because it revealed the internal heterogeneity of cancer tissue in terms of cytology, physiology and genetic informatics by extracting features from within and around the tumor [21]. Significant phenotypic differences in tumour region imaging can compensate for spatio-temporal heterogeneity that cannot be elucidated by clinical factors [22–24]

Thus, in this study, a prognostic combined model was constructed based on radiomics and clinical features that could accurately screen for suitable AC patients.

2. Methods and materials

2.1 Sample size

In the research, nine features were finally retained, and then the estimated sample size was at least 90 cases. For the sample size of the validation cohort, we performed power calculation by PASS, and found that the minimum sample size was 36. In our study, 140 patients (98 in the training cohort and 42 in the validation cohort) were enrolled to ensure that the study was fully analyzed.

2.2 Patients

This study was approved by the Ethics Committee of the Affiliated Hospital of Zunyi Medical University (Approval No.: KLLY-2020-012). A retrospective analysis was performed for non-metastatic NPC patients newly diagnosed at the Affiliated Hospital of Zunyi Medical University from February 2013 to December 2017. The eligibility criteria were as follows: a) histologically diagnosed undifferentiated, non-keratinized carcinoma; b) examinations were performed to determine staging (such as MRI scan); c) complete clinical data, including age, sex, Epstein-Barr virus DNA (EBV-DNA), and TNM stage (eighth edition of AJCC) were available; d) no other malignancies were present. The exclusion criteria were as follows: a) treatment before baseline MRI scan, such as radiotherapy, chemotherapy, immunotherapy and surgery; b) incomplete clinical data; c) artefacts, blurs, faults, and disordered slices in the MRI; e) MRI examination was performed in another hospital; f) non-standard treatment; g) other deaths except those caused by NPC before the end of follow-up. This workflow is shown in **Fig 1**.

2.3 MRI scan

A total of 140 patients received 1.5T head and neck MRI (GE, USA, TR:350ms, TE:10ms, 5mm thickness) at the Affiliated Hospital of Zunyi Medical University, including enhanced-MRI sequence, T1WI sequence, and T2WI Flair sequence.

2.4 Follow-up and clinical endpoint

In the first two years of follow-up, patients were examined by routine imaging methods every three months, every six months from the third year to the fifth year, and annually thereafter. The primary endpoint, 3-year recurrence or metastasis free survival (RMFS), defined as the time from the date of the first MRI to the date of recurrence or metastasis or to the date of the follow-up (the follow-up time was over 36 months). The 3-year cancer-specific survival (CSS) was analysed as a secondary endpoint and defined as the time between the date of the first MRI to the date of death due to NPC. If nasopharyngoscopy, head and neck MRI, PET/CT and other examinations mentioned the possibility of metastasis or recurrence, further examination (such as MRI or biopsy) was required to identify potential involved sites. If further examination results were negative, the patients were followed up with every three months for at least one year.

2.5 Collection of clinical data

The clinical data include age, sex, T stage, N stage (AJCC 8th edition), family history, ethnicity, treatment scheme, leukocytes, neutrophils, eosinophils, basophils, hemoglobin, red blood cells, platelets, albumin, prealbumin, alanine aminotransferase, aspartate aminotransferase, alkaline phosphatase, serum creatinine, blood urea nitrogen, EBV-DNA, survival status, and time to recurrence or metastasis.
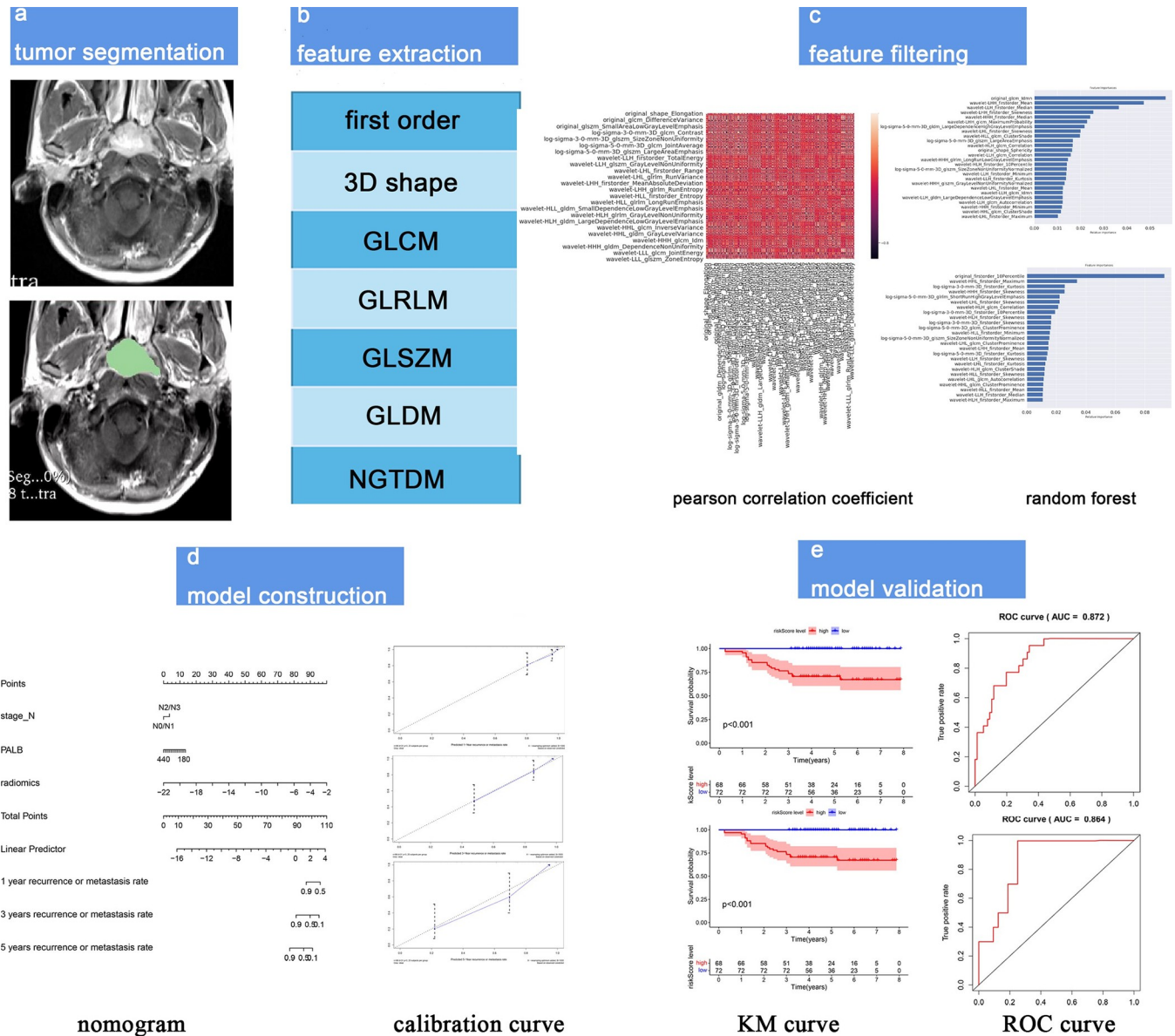
Fig 1. The workflow of radiomics nomogram establishment. a) Tumor segmentation in 3D-slicer; b) Seven types of features were extracted; c) Selection of features by pearson correlation coefficient (PCC) and random forest (RF); d) Radiomics nomogram construction and application; e) Evaluation and validation of models.

https://doi.org/10.1371/journal.pone.0287031.g001

2.6 Collection of image data

We obtained DICOM images (including T1WI, T2WI Flair, and enhanced-MRI sequences) directly from the picture archiving and communication system (PACS) system. The enhanced-MRI sequences were imported into "3D slicer" software, in which the whole region of interest (ROI) was drawn slice-by-slice to obtain the 3D segmented image. The tumor boundary was outlined mainly with reference to T2WI Flair and T1WI sequences. All images were segmented by two intermediate physicians with 10 years of experience and then reviewed by two associate chief physician who work in head and neck oncology.

2.7 Feature extraction and filtering

Features were extracted from the ROI using the Python "pyradiomics" package (implemented in Python, version 3.6). Image features include original image and filtered derived image.

We used intra- and interclass correlation coefficient (ICC) to assess the effects of variations in manual segmentation on radiomics feature values. ICC values greater than 0.75 indicate good agreement.

In order to avoid model overfitting, the extracted imaging features were filtered through the PCC and RF. PCC was used to assess the correlation between each pair of features. if correlation coefficient was greater than 0.7, one feature was excluded from each pair of correlated features (try to keep the original feature). Finally, we obtained the factors that were most closely associated with recurrence or metastasis.

2.8 Model construction

Eligible patients were randomly divided into a training cohort (n = 98) and an independent validation cohort (n = 42) in a ratio of 7:3. Both cohorts were well-balanced in baseline demographics and clinical factors by randomly grouping.

A clinical model (CM) was constructed for predicting the recurrence or metastasis of NPC. 1) Cox univariate analysis was performed by the clinical factors in the training cohort (clinical data included age, sex, EBV-DNA, platelet, ALP, ASP). 2) Construction of a Cox multivariate model with data from the training cohort. 3) Establishing a Receiver Operating Characteristic Curve (ROC) of 3-year recurrence or metastasis free rate (RMFR) to verify the sensitivity and specificity of the model. ROC curves were widely used to assess the sensitivity, specificity and accuracy of models [25, 26].

A radiomics model (RM) was constructed. 1) Cox univariate analysis in the training cohort was performed by the imaging features which selected by the PCC and the RF; 2) RM was constructed by Cox multivariate analysis; 3) A ROC of 3-year RMFR was established.

Cox multivariate regression analysis was performed on the clinical factors and imaging features that were statistically different from those obtained from the Cox univariate regression analysis, to constructed the clinical-radiomics model (CRM), and the Rad-scores were calculated. Similarly, the sensitivity and specificity of the model were verified by the ROC.

2.9 Evaluation and validation of models

The prediction models were constructed through the training cohort, and were verified in the verification cohort. We used the Delong test to compare the area under curves (AUCs) of the CRM with those of the CM and the RM respectively. Kaplan-Meier curves were plotted for the CRM with high-and low-risk groups. Log-rank test was used to test the difference of survival curves between high- and low-risk groups. The Rad-score was used to predict the recurrence or metastasis rate of NPC at 1, 3 and 5 years by nomogram, and the prediction efficiency of the model was verified by calibration curves.

2.10 Comparison of the survival benefit of patients with or without AC with subgroup analysis

The patients in two cohorts were stratified into high- and low-risk subgroups based on the median Rad-score of CRM. The comparison of the survival benefit of patients with or without AC was performed in the high- and low-risk subgroups by analyzing Kaplan-Meier survival curves.

2.11 Statistical analysis

We performed the clinical factors in the training and validation cohorts from the primary dataset using the Fisher's exact test and χ^2 tests. the RMFR and the CSS rate between the two groups were compared using log-rank test, and Kaplan-Meier curves were used to provide time-to-event data. All analysis were performed using SPSS 18.0 (https://www.ibm.com/spss), R 3.6.3 (http://www.R-project.org) and Python 3.6 (https://www.python.org/)). Two-sided p values < 0.05 were considered statistically significant.

3. Results

3.1 Patient characteristics

A total of 227 confirmed cases of NPC were collected in this study, and 140 patients were finally enrolled. (Patient screening flow chart is shown in **S1 Fig**). Median follow-up time of 140 patients was 61.36 months (range, 56.89–65.85; 41 patients had recurrence or metastasis, and 99 patients did not). There were no significant differences in sex, stage, treatment scheme and the number of people infected with EBV between the training cohort and the validation cohort. The 3-year RMRF of the training cohort and the validation cohort were 74.5% and 73.8%, respectively (P > 0.05). 3-year CSS was 90.8% in the training cohort and 81% in the validation cohort (P > 0.05). The characteristics of these patients are shown in **Table 1** and **Fig 2** [27–29].

3.2 Construction of the CM

The CM was constructed only from the clinical factors (24 clinical features, such as N stage, sex) of NPC. These results showed that PALB, N stage and alanine aminotransferase (AST) level were independent prognostic factors for recurrence or metastasis (**Table 2**) by the Cox univariate and multivariate analysis. Among them, PALB was a protective factor. The risk of N2/N3 was 4 times higher than that of N1/N0 patients. the risk of T3/T4 is 2.23 times higher than that of T1/T2 patients. T stage, N stage, PALB and AST were included in the subsequent construction of the CRM. However, EBV-DNA and adjuvant chemotherapy do not affect recurrence or metastasis in NPC (p > 0.05).

3.3 Construction of the RM

Feature extraction and filtering: A total of 960 features were extracted from head and neck enhanced-MRI on PyRadiomics platform by python, including six types (**Fig 1B**). The all features are described in S1 and S2 Tables. including 14 3D shapes, 242 Glcms, 154 Gldms, 176 Glrlms, 176 Glszms and 198 first order. The values of all features were normalized and limited to between 0 and 1 to reduce the variability of feature values (the method is described in S1 File). A total of 773 radiomics features had a good reliability with ICC > 0.75. In order to avoid model overfitting, after filtering out many features by PCC (**Fig 1C**), 25 and 26 imaging features respectively were selected by RF by using time and state of recurrence or metastasis as endpoints, respectively (**Fig 1C**). Forty-six features were selected, including wavelet-HLH_firstorder_Maximum, wavelet-LHL_glcm_ClusterProminence and so on, which were the union of two results obtained through RF.

Eleven features were associated with recurrence or metastasis finally by Cox univariate analysis. These eleven features were subjected by Cox multivariate regression analysis to construct a RM. Six features were independent prognostic factors. Among them, the features, original_glcm_Idmn and log_sigma_5_0_mm_3D_glszm_ SizeZoneNonUniformityNormalized, had an extremely negative impact on recurrence or metastasis (**Table 3**).

Table 1. Baseline tables for the training cohort and validation cohort.

	Training cohort	Validation cohort	p		Training cohort	Validation cohort	P
	98	42			98	42	
Age(years)			0.712	>4.73	25(25.5%)	12(26.4%)	
≤47	48.9(49%)	22(52.4%)		**Eosinophils, $\times10^9$/L**			0.461
>47	51.0(51%)	20(47.6%)		median (IQR) 0.135 (0.07–0.21)			
Sex			0.937	≤0.13	47(48.0%)	23(54.8%)	
man	67(68.4%)	29(69.0%)		>0.13	51(52.0%)	19(45.2%)	
women	31(31.6%)	13(31.0%)		**Basophilic, $\times10^9$/L**			0.732
EBV-DNA			0.955	median (IQR) 0.02 (0–0.04)			
positive	35(35.7%)	14(33.3%)		≤0.02	60(61.2%)	27(64.3%)	
negative	51(52.1%)	23(54.8%)		>0.02	38(38.8%)	15(35.7%)	
unmeasured	12(12.2%)	5(11.9%)		**Platelet, $\times10^9$/L**			
Nation			0.535	median (IQR) 227 (194–267)			0.07
ethnic Han	85(86.7%)	38(90.5%)		≤217	47(47.5%)	13(31.0%)	
minority	13(13.3%)	4(9.5%)		>217	52(52.5%)	29(69.0%)	
Family history			0.766	**Serum creatinine, umol/L**			
yes	10(10.2%)	5(11.9%)		median (IQR) 71 (60–79)			0.427
no	88(89.8%)	37(88.1%)		≤60	24(24.5%)	13(31.0%)	
T stage			0.461	>60	74(75.5%)	29(69.0%)	
T1\T2	51(52.0%)	19(45.2%)		**Blood urea nitrogen, mmol/L**			
T3\T4	47(47.9%)	23(54.8%)		median (IQR) 4.42 (3.55–5.7)			0.138
N stage			0.97	≤5	57(58.2%)	30(71.4%)	
N0\N1	40(40.8%)	17(40.5%)		>5	41(41.8%)	12(28.6%)	
N2\N3	58(59.2%)	25(59.5%)		**Albumin, g/L**			
Induction chemotherapy			0.283	median (IQR) 40.4 (38–54.3)			0.282
yes	93(94.9%)	37(88.1%)		≤40	51(52.0%)	26(61.9%)	
no	5(5.1%)	5(11.9%)		>40	47(48.0%)	16(38.1%)	
Adjuvant chemotherapy			0.891	**Prealbumin, mg/L**			
yes	20(20.4%)	9(21.4%)		median (IQR) 255 (213–292.5)			0.937
no	78(79.6%)	33(78.6%)		≤255	51(52.1%)	20(47.6%)	
Concurrent chemoradiotherapy			1	>255	47(47.9%)	22(52.4%)	
yes	90(91.8%)	39(92.9%)		**Alanine aminotransferase**			
no	8(8.2%)	3(7.1%)		median (IQR) 18.5 (14–30)			0.843
The first blood sample after diagnosis				≤19	61(68.4%)	28(67.9%)	
Red blood cell, $\times10^{12}$/L				>19	37(31.6%)	14(32.1%)	
median (IQR) 4.66 (4.35–4.96)			0.478	**Alkaline phospholipase, U/L**			0.902
≤5.1	84(85.7%)	34(80.9%)		median (IQR) 83 (67.75–94)			
>5.1	14(14.3%)	8(19.1%)		≤92	71(72.4%)	30(71.4%)	
Hemoglobin, g/L				>92	27(27.6%)	12(28.6%)	
median (IQR) 141 (129.75–150)			0.483	**Aspartate aminotransferase, U/L**			0.112
≤140	45(45.9%)	22(54.2%)		median (IQR) 22 (19–28)			
>140	84(85.8%)	20(74.6%)		≤24	56(57.1%)	30(71.4%)	
White blood cell, $\times10^9$/L				>24	42(42.9%)	12(28.6%)	
median (IQR) 6.035 (4.99–7.38)			0.683	**Survival state**			0.169
≤7.13	69(70.4%)	31(73.8%)		live	86(87.8%)	33(78.6%)	
>7.13	29(29.6%)	11(26.2%)		dead	12(12.2%)	9(21.4%)	
Neutrophil, $\times10^9$/L			0.707	**Recurrence or metastasis state**			0.358

(Continued)

Table 1. (Continued)

	Training cohort	Validation cohort	p		Training cohort	Validation cohort	P
median (IQR) 3.73 (2.99–4.78)				no	67(68.4%)	32(76.2%)	
≤4.73	73(74.5%)	30(73.6%)		yes	31(31.6%)	10(23.9%)	

P-value <0.05 indicated a significant difference. Both cohorts were well balanced in baseline demographic and clinical characteristics. Statistical comparisons between the training and validation cohorts were computed using the $\chi 2$ test for categorical variables.

https://doi.org/10.1371/journal.pone.0287031.t001

3.4 Construction of the CRM

It can be seen from the above results that four clinical factors and eleven imaging features were statistically different by Cox univariate analysis. We then constructed a CRM consisting of nine features (seven imaging features and two clinical factors) by Cox multivariate regression analysis. We calculated the Rad-score for each patient using the formula resulting from the 9 features weighted by their regression coefficients as follows: Risk score = —(3.977 × *wavelet_LHH_firstorder_Skewness*)—(4.794 × *log_sigma_3_0_mm_3D_firstorder_10Percentile*)– (5.583 × *wavelet-LHL_firstorder_Skewness*)—(9.460 × *log-sigma-5-0-mm-3D_glszm_SizeZone-NonUniformityNormalized*) + (6.459 × *original_glcm_Idmn*) + (1.462 × *wavelet_LLH_glcm_Autocorrelation*)—(6.665× *wavelet-LHH_firstorder_Mean*) + 0.726 × N2/N3–0.01 × PALB. Based on median Rad-score, 68 patients were classified as high-risk group (Rad-score >2.03) and 72 as low-risk group (Rad-score ≤2.03).

3.5 Evaluation and validation of models

The median Rad-score divided patients into high- and low-risk groups. The AUCs of the training cohort and validation cohort based on CM were 0.775 (p < 0.001, 95% CI, 0.683–0.867) and 0.697 (p = 0.06, 95% CI, 0.498–0.896), respectively. the sensitivities were 0.742 and 0.600, and the specificities were 0.672 and 0.844, respectively (**Fig 3A and 3B**); The AUCs of the
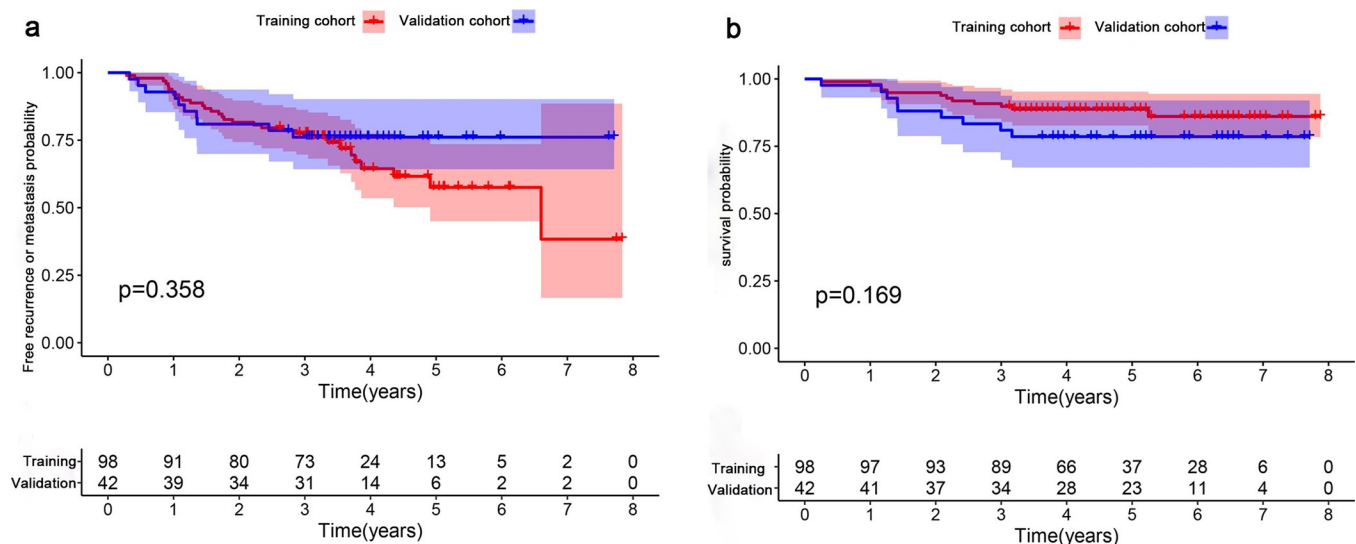
Fig 2. KM curves of training cohort and validation cohort. a) The KM curves of patients with the RMFS, 3-year RMFR were 74.5% and 73.8% in training and validation cohorts, respectively (p>0.05); b) The KM curves of patient's CSS in training cohort and validation cohort. The 3-year CSS rates were 90.8% and 81%, respectively (p>0.05). P≥0.05 indicates no statistically significant difference between the two groups.

https://doi.org/10.1371/journal.pone.0287031.g002

Table 2. The Cox univariate and multivariate analysis for clinical characteristics.

id	Univariate analysis				Multivariate analysis			
	HR	HR.95L	HR.95H	pvalue	coef	HR.95L	HR.95H	pvalue
PALB	0.989	0.982	0.995	**0.001**	-0.010	0.982	0.997	**0.009**
N stage (N2/N3 vs. N0/N1)	4.016	1.779	9.069	**0.001**	1.115	1.226	7.587	**0.016**
T stage (T3/T4 vs. T1/T2)	2.230	1.169	4.254	**0.015**	-	-	-	-
AST	1.018	1.002	1.034	**0.023**	0.015	1.000	1.030	**0.049**
PLT	0.995	0.989	1.000	0.071	-	-	-	-
Neutrophil	1.169	0.969	1.411	0.102	-	-	-	-
sex (female vs. male)	0.555	0.265	1.164	0.119	-	-	-	-
adjuvant (yes vs. no)	0.537	0.209	1.377	0.195	-	-	-	-
age	1.016	0.990	1.044	0.231	-	-	-	-
WBC	1.099	0.941	1.285	0.234	-	-	-	-
AlB	0.953	0.874	1.039	0.275	-	-	-	-
basophilic	0.003	0.000	534.878	0.348	-	-	-	-
APL	1.007	0.992	1.022	0.358	-	-	-	-
RBC	0.744	0.382	1.449	0.384	-	-	-	-
crearinine	0.990	0.968	1.013	0.412	-	-	-	-
HB	0.993	0.973	1.014	0.515	-	-	-	-
family history (yes vs. no)	1.333	0.474	3.746	0.586	-	-	-	-
nation (minority vs. Han)	0.789	0.281	2.218	0.653	-	-	-	-
EBV-DNA (positive vs. negative)	1.112	0.563	2.200	0.759	-	-	-	-
ALT	0.997	0.974	1.020	0.769	-	-	-	-
BUN	1.027	0.825	1.280	0.810	-	-	-	-
Eosnophils	0.923	0.131	6.490	0.936	-	-	-	-

P-value <0.05 indicated a significant difference. N stage and AST were regarded as independent prognostic factors. HR, Hazard ratio. CI,confidence interval.

https://doi.org/10.1371/journal.pone.0287031.t002

training cohort and validation cohort based on RM were 0.844 (p < 0.001, 95% CI, 0.764–0.924) and 0.807 (p = 0.003,95% CI, 0.672–0.942), respectively. the sensitivities were 0.903 and 0.900, and the specificities were 0.672 and 0.687, respectively (**Fig 3C and 3D**), respectively.

Table 3. The Cox univariate and multivariate analysis for imaging factors.

id	Univariate analysis				Multivariate analysis			
	HR	95L	95H	pvalue	coef	95L	95H	pvalue
log_sigma_3_0_mm_3D_firstorder_10Percentile	5.815	1.195	28.286	**0.029**	-4.352	2.193E-04	0.757	**0.036**
log_sigma_5_0_mm_3D_firstorder_Kurtosis	5.161	1.385	19.229	**0.014**	-	-	-	-
log_sigma_5_0_mm_3D_glszm_SZNUN	0.038	0.004	0.378	**0.005**	-9.358	1.791E-07	0.042	**0.003**
original_glcm_Idmn	209.697	5.263	8355.602	**0.004**	8.065	2.232	4.532E+06	**0.030**
wavelet_HHH_glrlm_LRLGLE	0.025	0.001	0.760	**0.034**	-	-	-	-
wavelet_HHL_firstorder_Maximum	4.759	1.076	21.054	**0.040**	-	-	-	-
wavelet_LHH_firstorder_Mean	0.066	0.005	0.783	**0.031**	-6.272	0.000	0.325	**0.017**
wavelet_LHH_firstorder_Skewness	0.055	0.006	0.518	**0.011**	-5.074	0.000	0.188	**0.003**
wavelet_LHL_firstorder_Skewness	0.030	0.002	0.431	**0.010**	-4.881	0.000	0.198	**0.003**
wavelet_LLH_firstorder_Median	32.487	2.854	369.791	**0.005**	-	-	-	-
wavelet_LLH_glcm_Autocorrelation	4.966	1.171	21.054	**0.030**	1.503	0.813	24.875	0.085

P-value <0.05 indicated a significant difference. eleven radiomic features were related to recurrence or metastasis, including 6 independent prognostic features. HR, Hazard ratio. CI, confidence interval. SZNUN, SizeZoneNonUniformityNormalized. LRLGLE, LongRunLowGrayLevelEmphasis.
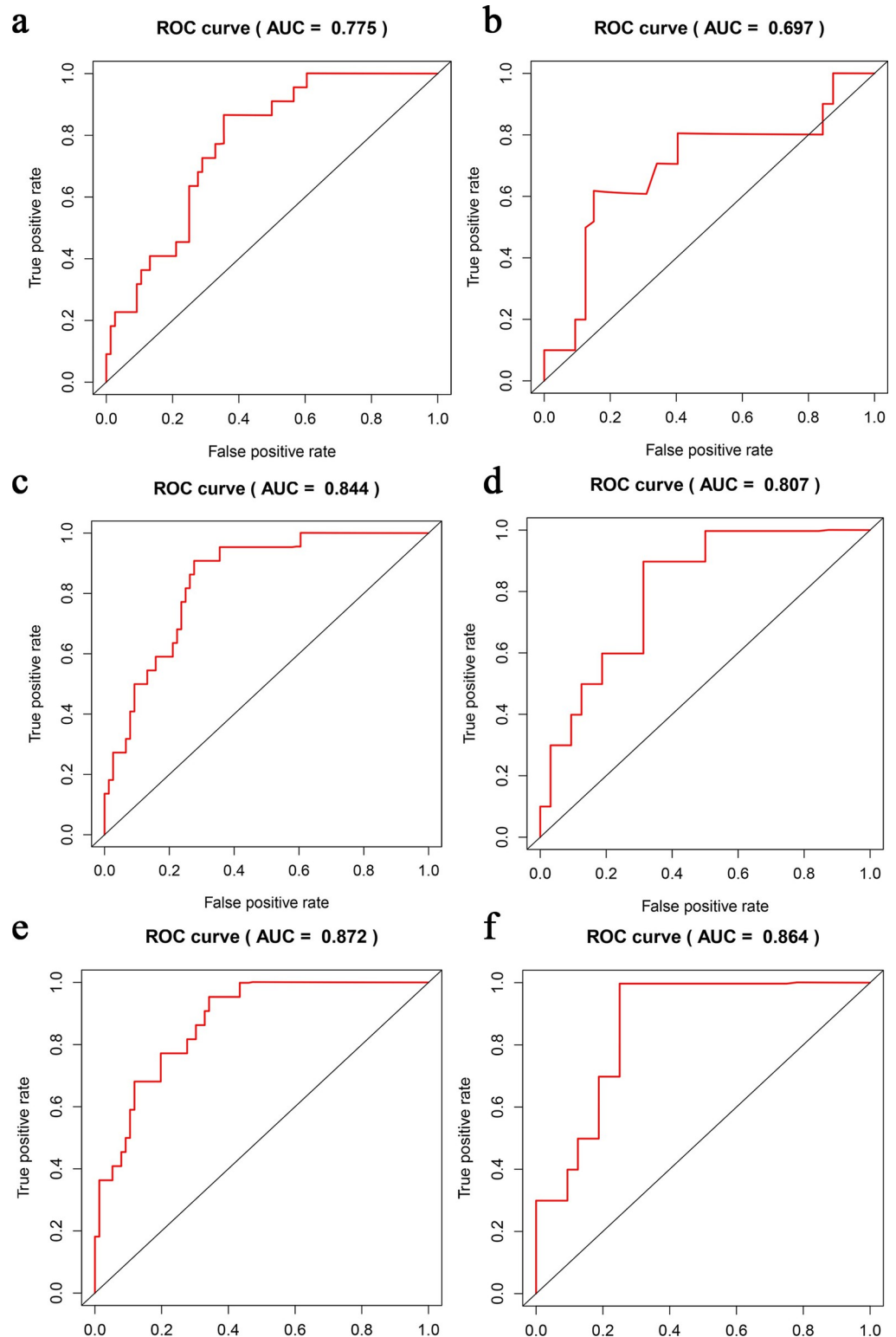
https://doi.org/10.1371/journal.pone.0287031.t003

Fig 3. ROCs of the three models. a), c) and e) were the training cohort; b), d) and f) were the validation cohort; a) and b) were the ROCs of the CM, with AUCs of 0.775 (p < 0.001, 95% CI: 0.683–0.867) and 0.697 (p = 0.06,95% CI: 0.498–0.896), respectively; c) and d) ROCs of the RM, with AUCs of 0.844 (p < 0.001, 95% CI, 0.764–0.924) and 0.807 (p = 0.003,95% CI, 0.672–0.942), respectively; e) and f) ROCs of the CRM, with AUCs of 0.872 (p<0.001,95% CI, 0.805–0.939) and 0.864 (p = 0.001,95% CI, 0.756–0.972), respectively.

https://doi.org/10.1371/journal.pone.0287031.g003

Based on CRM, the training cohort's AUC was 0.872 (p<0.001,95% CI, 0.805–0.939), the sensitivity and specificity were 0.935 and 0.672; the validation cohort's AUC was 0.864 (p = 0.001, 95% CI, 0.756–0.972), the sensitivity and specificity were 1 and 0.75, respectively. The CRM showed a very good predictive power (**Fig 3E and 3F**). The DeLong test showed the statistical significance between the CM and the CRM in the training cohort (p<0.05). There was no significant difference between the AUC of the combined RM and CRM in the training and validation cohorts (DeLong test).

Most NPC recurrence or metastasis within 3 years. The 3-year RMFR were 54.5% in the high-risk group and 96.2% in the low-risk group (p <0.001) (**Fig 4A**), and the 3-year cancer specific survival (CSS) rates were 75% in the high-risk group (p<0.001) (**Fig 4B**). A nomogram was generated based on CRM (**Fig 4C**). Calibration curves showed good fitness for the CRM (**Fig 4D**) that can accurately predict the prognosis of NPC.

3.6 For different treatment schemes, the prediction performance of CRM

For LA-NPC, the treatment schemes vary from place to place, especially whether to add AC. To further determine whether the CRM was suitable for the induction with concurrent chemoradiotherapy (IC+CCRT) and the induction, concurrent chemoradiotherapy and adjuvant chemotherapy (IC+CCRT+AC), we calculated AUCs for different patients who received IC + CCRT only, patients who received IC + CCRT + AC, and all enrolled patients. We found that the CRM predicted the 3-year RMFR of patients with IC+CCRT with an AUC of 0.866 (p<0.001, 95% CI, 0.795–0.936); At the same time, in IC+CCRT+AC group, the AUC was 0.806 (p = 0.013, 95% CI, 0.645–0.936) (**Fig 5A and 5B**), and high sensitivity and specificity were achieved in both groups (**Table 4**). The model had high accuracy for both treatment schemes.

3.7 Only the high-risk patients in the CMR were recommended adjuvant chemotherapy (AC)

Not all patients with NPC are suitable for AC. After adding AC to some patients, the toxicity and cost increased, and there was no obvious survival benefit [5, 30]. Therefore, it is necessary to explore which patients are suitable for AC. We explored the efficacy of AC in patients in the high- and low-risk groups respectively. The results showed that in the high-risk group, the 3-year RMFR of patients who received AC was 78.6%, and the 3-year RMFR of patients who did not receive AC was only 48.1% (p = 0.03). In the low-risk group, the 3-year RMFR was not significant difference (p = 0.26) (**Fig 5C and 5D**). It was suggested that for high-risk patients, the combination of AC may should be recommended. For low-risk patients, AC was not recommended because of no benefit and increased toxicity. The model was able to filter patients who would benefit from AC. (Examples: in some high-risk patients, no recurrence or metastasis were found after AC, and recurrence was found after no AC **Fig 5E**)

4. Discussion

In fact, AC remains a controversial treatment because previous study failed to demonstrate clinical effectiveness [5, 31]. Chan et al. found that, in patients with NPC with detectable post-RT plasma EBV DNA, AC with cisplatin and gemcitabine did not improve relapse-free survival (49.3% vs. 54.7%; P = 0.75) [31]. However, Tao et al. revealed that there were differences between the IC+CCRT and IC+CCRT+ AC groups in terms of the 5-year overall survival (OS) (78.9% vs. 85.0%, P = 0.034), disease-free survival (DFS) (73.4% vs. 81.7%, P = 0.029), and distant metastasis-free survival (DMFS) (84.9% vs. 76.0%, P = 0.019) in N2/3 positive NPC patients [11]. Why the results were opposite? The biggest reason is that many studies did not
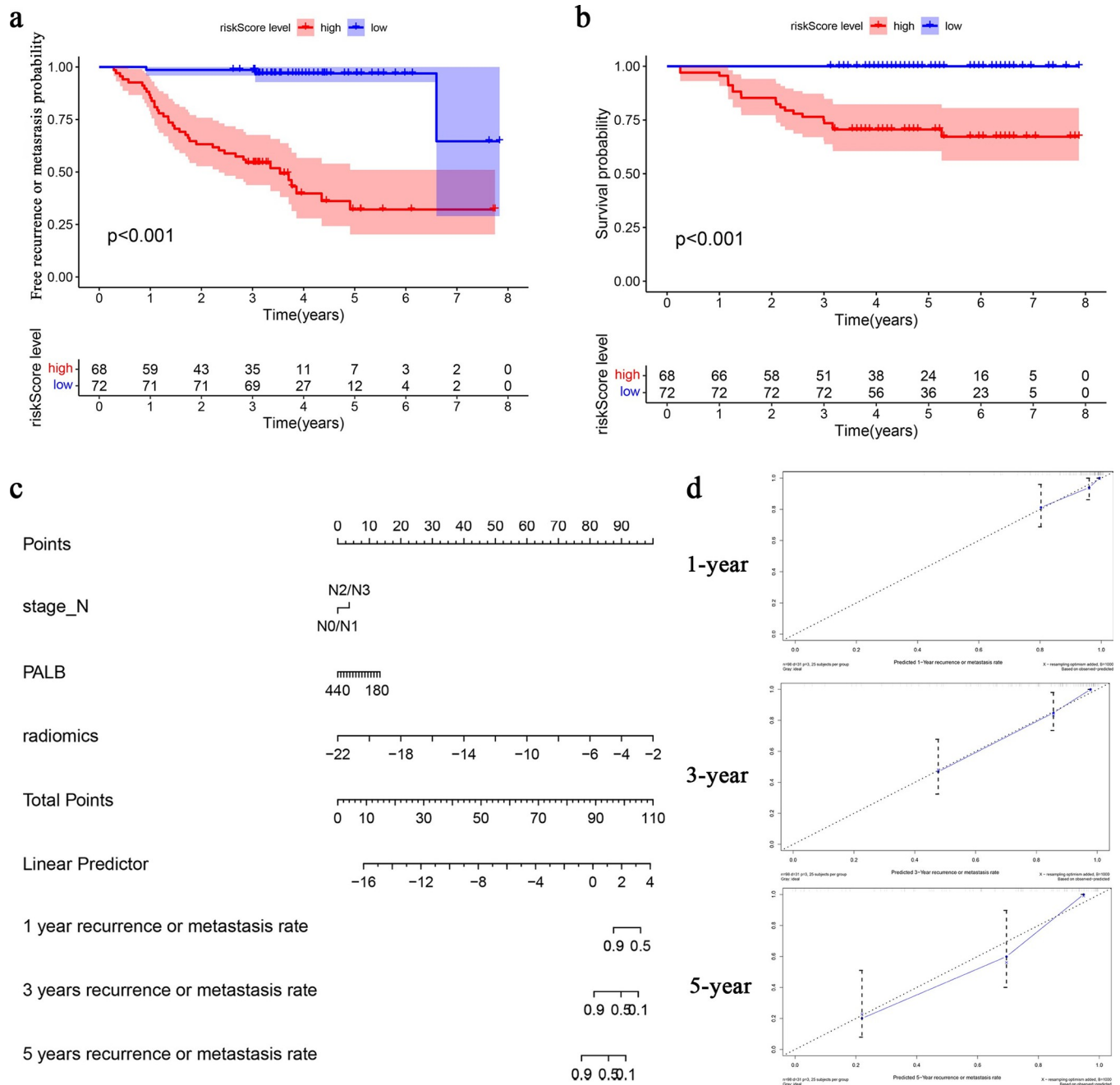
Fig 4. Evaluation and validation of the CRM. a) Kaplan-Meier survival curve for 3-year RMFR. the RMFR in the high-risk group was significantly lower than that in the low-risk group (54.5% vs 96.2%, P<0.001); b) Kaplan-Meier survival curve for the 3-year CSS rates. The 3-year CSS rates were 75% for the high-risk (P <0.001); c) Nomogram predicted the 1-, 3- and 5-year RMFRs of patients with NPC; d) the calibration curves of the 1-, 3-, 5-year recurrence or metastasis, respectively (RM, recurrence or metastasis).

https://doi.org/10.1371/journal.pone.0287031.g004

stratify patients. Hui et al. constructed a risk prediction model to integrate postradiotherapy EBV-DNA and TNM stage for risk stratification of NPC patients after completion of radio-/chemoradiotherapy to AC or observation. The findings showed that AC in low-risk group did not benefit and increases toxicities. But the limitation was that the model could not predict the survival benefits from adjuvant chemotherapy in high-risk group [32]. In addition, Shen et al.
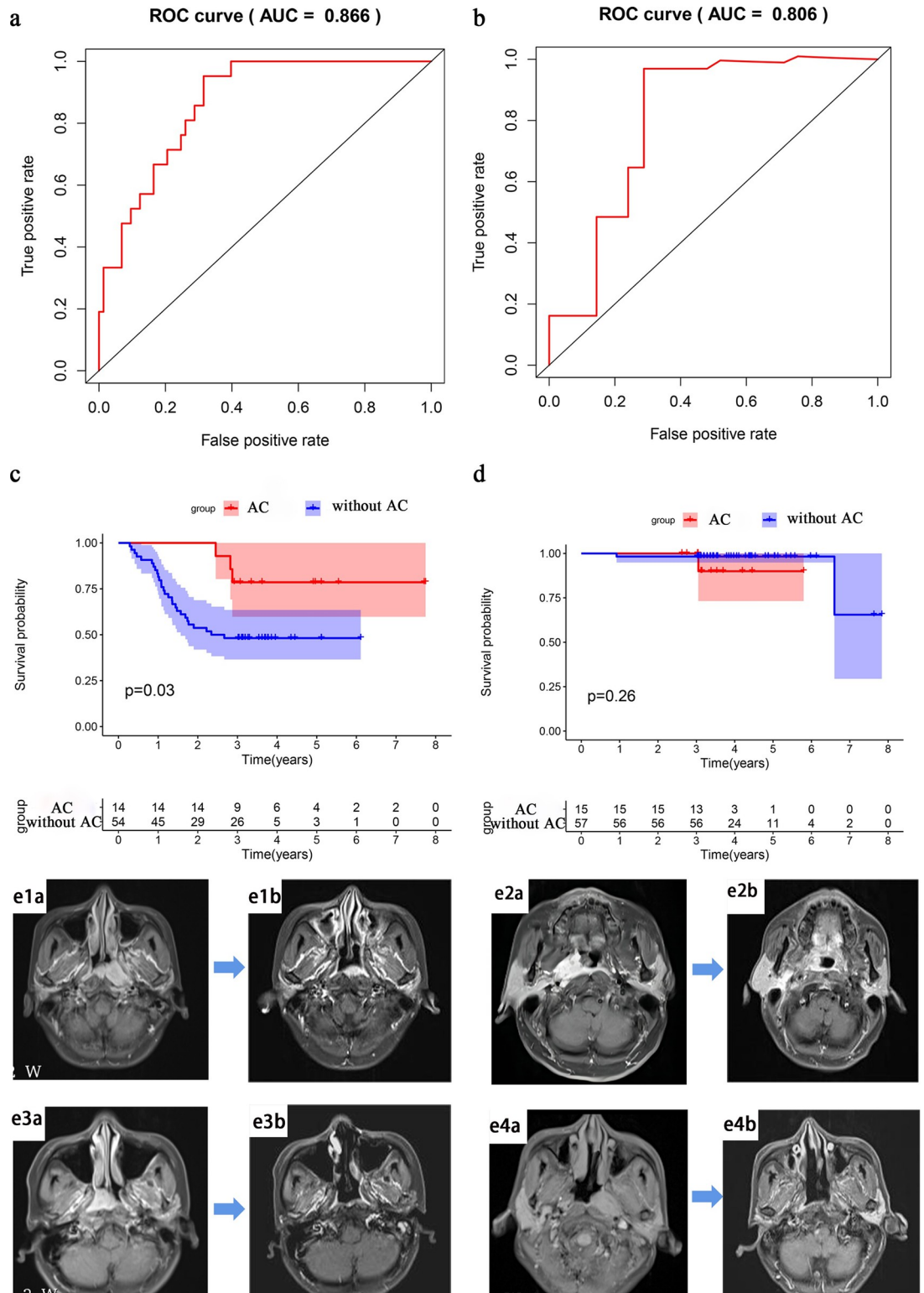
Fig 5. Subgroup analysis of the CRM. a) The group of the IC + CCRT scheme (AUC = 0.866 P<0.001); b) The group of the IC + CCRT + AC scheme (AUC = 0.806 P = 0.013). c) In the high-risk group, the 3-year RMFR of patients receiving AC was significantly higher than the 3-year RMFR of patients not receiving adjuvant chemotherapy (P = 0.03); d) In the low-risk group, the 3-year RMFRs were not statistically significant (P = 0.26); e) Example, In some high-risk patients, e1a), e2a), e3a), e4a) The MRI at initial diagnosis; e1b), e2b) Recurrence was detected by MRI within 3 years of treatment in patients who did not receive

adjuvant chemotherapy; e3b), e4b) No recurrence was detected by MRI within 3 years of treatment in patients who received adjuvant chemotherapy.

found that in the high-risk group derived from radiomic scoring, CCRT+AC achieved significantly better PFS, LRRFS, DMFS and OS than IC+CCRT. In the low-risk group, IC+CCRT yielded significantly better outcomes than CCRT+AC [33]. It is necessary to identify patients who may benefit more from AC to reduce side effects and unnecessary costs. In this study, we constructed a CRM to predict the 3-year RMFR in NPC patients based on MRI radiomics and clinical factors. The CRM could divide patients into the high-risk and low-risk groups. More importantly, AC could improve 3-year RMFR in high-risk patients in CRM.

I compared the predictive performance to previous studies on the same data. It was found that the AUC values of our model were higher in both the training and validation cohort (S2 Fig) [34–36], but these results contain more features and sequences. In our study, the CRM showed higher predictive performance than CM, in both the training and the validation cohorts. Similar to our results, these studies found that MRI radiomics combined with clinical factors has better predictive power than that of traditional TNM staging in predicting the PFS and OS of NPC [37–39]. The main reason is that radiomics transforms the image into data information visible to the naked eye by extracting the features of the internal and surrounding tissues of the tumour, thereby revealing the internal heterogeneity of cancer tissue such as cytology, physiology and genetic informatics [21]. Texture features are mathematical parameters computed from the distribution of pixels, which can represent the heterogeneity of voxel arrangement in the tumour area [40]. The above point confirmed the result that there was no significant difference between the AUC of the RM and CRM in the training and validation cohorts (DeLong test). This was the reason why CM performs well in predicting RMFR in patients [41].

Finally, our CRM included 7 imaging features. Among these factors, we identified a powerful feature, original-glcm-Idmn. Idmn is also called the inverse difference moment normalized, which reflects the homogeneity of the image texture and measures the local change of the image texture. original-glcm-Idmn is a widely extracted texture feature, and may be positively correlated with NPC recurrence or metastasis [19]. Wavelet features reflect tumor information from eight spatial domains, and the "skewness" in wavelet subspace shows that tumor heterogeneity described by entropy and tumor intensity has prognostic value in high dimensional wavelet and logarithmic space [42]. In addition to, skewness was highly important in the RM by the study of Fan. The findings showed that luminal A had lower values of skewness and kurtosis features compared with luminal B in breast cancer. And, among the different prognostic models constructed by different combinations of features and clinical factors, only these two characteristics appeared most frequently [43].

Among the steps in radiomics, the most important steps are feature selection and model building. The limitation is that most feature extraction methods are low-quality and complex,

Table 4. The AUC values, sensitivity and specificity of the different treatment modes in CRM.

	AUC (95% CI)	P value	sensitive	specificity
IC+CCRT	0.866 (0.795–0.936)	<0.001	0.926	0.801
IC+CCRT+AC	0.806 (0.644–0.968)	0.013	1.000	0.632
all patients	0.869 (0.812–0.926)	<0.001	0.951	0.687

P-value <0.05 indicated a significant difference. IC+CCRT, induction combined with concurrent chemoradiotherapy; IC+CCRT+AC: induction, concurrent chemoradiotherapy and adjuvant chemotherapy.

and the results are not convincing. We filter features by PCC and RF and build the model by Cox multivariate regression analysis. The AUCs of the training and validation cohorts of the CRM were 0.872 (p<0.001,95% CI, 0.805–0.939), and 0.864 (p = 0.001,95% CI, 0.756–0.972), respectively. The AUCs were higher than that of the models built by logistic regression after filtering features by other statistical methods such as absolute shrinkage and selection operator (LASSO) (AUC, 0.7–0.8) [44]. RF, as a statistical method with high classification accuracy and efficiency, has high prognostic performance and good stability to data fluctuations. the data dimensionality was reduced by random forest, which is a good filtering method to solve model overfitting [45]. Zhang et al. found that the consistency index (c-index) values of the model constructed by RF screening features were about 0.82 in both internal and external validation cohorts [20]. PCC is the most commonly used statistical tool to reflect the degree of linear correlation between two variables and reduce the factors that influence each other [46]. Li et al. used radiomics to predict the prognosis of cervical cancer and selected the features by the PCC, and the c-index value of the model was also around 0.75 [47]. In addition to LASSO, many studies filtered features such as L1-logistic regression method and built models with support vector machine (SVM), which can also predict the prognosis, and their C-index and AUCs were about 0.7–0.8 [48–50].

The CRM included 2 clinical factors (N stage and PALB). In clinical stage, only N stage was included in the final combination model, excluding T stage. Possibly because T stage represents the size of the tumour and extent of invasion, and has little correlation with the microinvasion of the tumour, which was consistent with the results of some clinical studies [48, 51]. PALB was a positive factor in our study. The reason may be related to nutrition. Li et al. also found a positive correlation between ALB measurements and the overall survival rate [52]. EBV-DNA, as an early screening and prognostic indicator, should theoretically be associated with recurrence or metastasis [53–55]. In addition, Hu et al. found that AC might reduce the incidence of locoregional recurrence or distant metastasis in patients without post-radiotherapy plasma EBV DNA clearance [32]. However, in this study, EBV-DNA was not a predictive factor, which may be because thirty percent of the patients were not tested for EBV-DNA or because we performed only qualitative testing instead of quantitative testing.

In a 2012 study, Chen et al. found that AC may only increase toxicity. However, in recent years, they have also found that adjuvant capecitabine could improve outcomes in a specific population [5, 56]. Many studies found that the addition of AC in N2/3 patients can further improve the OS, DFS, and PFS, and the side effects were acceptable [11, 12]. Therefore, we need to stratify patients with NPC and look for patients who can benefit from AC. Several studies have accurately predicted the prognosis of IC by radiomics and selected patients suitable for induction chemotherapy [57–59]. Similarly, Keek et al. predicted the risk of local recurrence and distant metastases after CCRT by radiomics for patients with squamous carcinoma of the head and neck [60]. However, the most controversial aspect of AC has been less studied. Our final model accurately stratified NPC patients by radiomics and clinical factors. We found that in the high-risk group (Rad-score >2.03), the 3-year RMFR of patients receiving AC was significantly higher than that of patients without AC (p = 0.03), suggesting that for high-risk patients, combined AC was more recommended. In the low-risk group, the result showed that there was no statistical difference in 3-year RMFR regardless of whether they received AC or not. But for low-risk patients who received AC, the cumulative effect of chemotherapy lead to increased side effects (such as stomatitis, leucopenia) [5], decreased quality of life, and increased cost-effectiveness [30], which may suggest that combined AC was not applicable for low-risk patients [5].

Our study also had some limitations. First, only the phase with the most obvious enhanced MRI was selected for analysis. Further requests should be made for T1WI, T2WI and DWI

images. Second, the metastatic lymph nodes are also an important prognostic factor in NPC. Therefore, prognosis may be more accurately predicted by extracting metastatic lymph node region (GTVnd) and gross tumor volume (GTV). Third, we lacked external validation. Further external validation is required to improve diagnostic accuracy, sensitivity and specificity before clinical application of CRM [61, 62].

5. Conclusion

In conclusion, the accurate predictive model provided a noninvasive way to predict the outcomes of NPC and helped identify high-risk patients who benefited from AC for improve the 3-year RMFR. AC might not be necessary for low-risk patients.

Supporting information

S1 Fig. Patient screening flow chart.
(PNG)

S2 Fig. Comparison of AUC values between other studies and our study ROC curves.
(TIF)

S1 Table. Features extracted from targets outlined by an associate chief physician.
(XLSX)

S2 Table. Features extracted from targets outlined by another associate chief physician.
(XLSX)

S1 File. Other supplementary materials.
(DOCX)

S2 File. Supplementary material_code.
(DOCX)

Author Contributions

Conceptualization: Cheng Chen, Qing Luo.

Data curation: Qiaoyuan Wu, Yonghu Chang, Heng Liu, Hui Dong, Cheng Chen, Qing Luo.

Formal analysis: Qiaoyuan Wu, Hui Dong, Qing Luo.

Funding acquisition: Qing Luo.

Methodology: Qiaoyuan Wu, Cheng Yang, Cheng Chen.

Resources: Cheng Chen, Qing Luo.

Software: Cheng Yang.

Validation: Cheng Yang, Fang Chen.

Writing – original draft: Qiaoyuan Wu, Fang Chen.

References

1. Chen Y-P, Chan ATC, Le Q-T, Blanchard P, Sun Y,Ma J. Nasopharyngeal carcinoma. The Lancet. 2019; 394(10192): 64–80. https://doi.org/10.1016/s0140-6736(19)30956-0 PMID: 31178151

2. Sung H, Ferlay J, Siegel RL, Laversanne M, Soerjomataram I, Jemal A, et al. Global Cancer Statistics 2020: GLOBOCAN Estimates of Incidence and Mortality Worldwide for 36 Cancers in 185 Countries.

CA: A Cancer Journal for Clinicians. 2021; 71(3): 209–249. https://doi.org/10.3322/caac.21660 PMID: 33538338

3. Lee AW, Ng WT, Chan LL, Hung WM, Chan CC, Sze HC, et al. Evolution of treatment for nasopharyngeal cancer—success and setback in the intensity-modulated radiotherapy era. Radiother Oncol. 2014; 110(3): 377–384. https://doi.org/10.1016/j.radonc.2014.02.003 PMID: 24630534

4. Guan H, He Y, Wei Z, Wang J, He L, Mu X, et al. Assessment of induction chemotherapy regimen TPF vs GP followed by concurrent chemoradiotherapy in locally advanced nasopharyngeal carcinoma: A retrospective cohort study of 160 patients. Clinical Otolaryngology. 2019; 45(2): 274–279. https://doi.org/10.1111/coa.13489 PMID: 31788988

5. Chen L, Hu C-S, Chen X-Z, Hu G-Q, Cheng Z-B, Sun Y, et al. Concurrent chemoradiotherapy plus adjuvant chemotherapy versus concurrent chemoradiotherapy alone in patients with locoregionally advanced nasopharyngeal carcinoma: a phase 3 multicentre randomised controlled trial. The Lancet Oncology. 2012; 13(2): 163–171. https://doi.org/10.1016/S1470-2045(11)70320-5 PMID: 22154591

6. Tang LL, Chen YP, Chen CB, Chen MY, Chen NY, Chen XZ, et al. The Chinese Society of Clinical Oncology (CSCO) clinical guidelines for the diagnosis and treatment of nasopharyngeal carcinoma. Cancer Commun (Lond). 2022; 41(11): 1195–1227. https://doi.org/10.1002/cac2.12218 PMID: 34699681

7. Bossi P, Chan AT, Licitra L, Trama A, Orlandi E, Hui EP, et al. Nasopharyngeal carcinoma: ESMO-EURACAN Clinical Practice Guidelines for diagnosis, treatment and follow-up(dagger). Ann Oncol. 2021; 32(4): 452–465. https://doi.org/10.1016/j.annonc.2020.12.007 PMID: 33358989

8. Pfister DG, Spencer S, Adelstein D, Adkins D, Anzai Y, Brizel DM, et al. National Comprehensive Cancer Network (NCCN) guidelines. Head and Neck Cancers, Version 3, 2021. J Natl Compr Canc Netw. 2021; 18(7): 873–898. https://doi.org/10.6004/jnccn.2020.0031 PMID: 32634781

9. Zhou L, Lin J, Chen J,Zhang S. Induction plus adjuvant chemotherapy, combined treatment with nimotuzumab, and intensity-modulated radiation therapy for N3 stage nasopharyngeal carcinoma: A pilot study. J Cancer Res Ther. 2021; 17(7): 1730–1735. https://doi.org/10.4103/jcrt.jcrt_2145_21 PMID: 35381746

10. Wang P, Dong F, Cai C,Ke C. Treatment outcomes of induction chemotherapy combined with intensity-modulated radiotherapy and adjuvant chemotherapy for locoregionally advanced nasopharyngeal carcinoma in Southeast China. Medicine (Baltimore). 2021; 100(33): 1–5. https://doi.org/10.1097/MD.0000000000027023 PMID: 34414997

11. Tao HY, Liu H, He F, He CX, Li R, Du KP, et al. Adjuvant chemotherapy following combined induction chemotherapy and concurrent chemoradiotherapy improves survival in N2-3-positive nasopharyngeal carcinoma patients. J Cancer Res Clin Oncol. 2021, 10.1007/s00432-021-03846-6: https://doi.org/10.1007/s00432-021-03846-6 PMID: 34822015

12. Niu X, Xue F, Liu P, Hu C,He X. Long-term outcomes of induction chemotherapy followed by intensity-modulated radiotherapy and adjuvant chemotherapy in nasopharyngeal carcinoma patients with N3 disease. Transl Oncol. 2021; 14(12): 1–7. https://doi.org/10.1016/j.tranon.2021.101216 PMID: 34530195

13. Kumar V, Gu Y, Basu S, Berglund A, Eschrich SA, Schabath MB, et al. Radiomics: the process and the challenges. Magn Reson Imaging. 2012; 30(9): 1234–1248. https://doi.org/10.1016/j.mri.2012.06.010 PMID: 22898692

14. Dalal V, Carmicheal J, Dhaliwal A, Jain M, Kaur S,Batra SK. Radiomics in stratification of pancreatic cystic lesions: Machine learning in action. Cancer Lett. 2020; 469: 228–237. https://doi.org/10.1016/j.canlet.2019.10.023 PMID: 31629933

15. Liu S, Yu X, Yang S, Hu P, Hu Y, Chen X, et al. (2021) Machine Learning-Based Radiomics Nomogram for Detecting Extramural Venous Invasion in Rectal Cancer. Front Oncol. 2021; 11: e610338. https://doi.org/10.3389/fonc.2021.610338 PMID: 33842316

16. Li H, Gao L, Ma H, Arefan D, He J, Wang J, et al. Radiomics-Based Features for Prediction of Histological Subtypes in Central Lung Cancer. Front Oncol. 2021; 11: e658887. https://doi.org/10.3389/fonc.2021.658887 PMID: 33996583

17. Bai X, Huang Q, Zuo P, Zhang X, Yuan J, Zhang X, et al. MRI radiomics-based nomogram for individualised prediction of synchronous distant metastasis in patients with clear cell renal cell carcinoma. Eur Radiol. 2021; 31(2): 1029–1042. https://doi.org/10.1007/s00330-020-07184-y PMID: 32856163

18. Romeo V, Cuocolo R, Apolito R, Stanzione A, Ventimiglia A, Vitale A, et al. Clinical value of radiomics and machine learning in breast ultrasound: a multicenter study for differential diagnosis of benign and malignant lesions. Eur Radiol. 2021, 10.1007/s00330-021-08009-2: https://doi.org/10.1007/s00330-021-08009-2 PMID: 34018057

19. Zhang L, Dong D, Li H, Tian J, Ouyang F, Mo X, et al. Development and validation of a magnetic resonance imaging-based model for the prediction of distant metastasis before initial treatment of

nasopharyngeal carcinoma: A retrospective cohort study. EBioMedicine. 2019; 40: 327–335. https://doi.org/10.1016/j.ebiom.2019.01.013 PMID: 30642750

20. Zhang F, Zhong LZ, Zhao X, Dong D, Yao JJ, Wang SY, et al. A deep-learning-based prognostic nomogram integrating microscopic digital pathology and macroscopic magnetic resonance images in nasopharyngeal carcinoma: a multi-cohort study. Ther Adv Med Oncol. 2020; 12: 1–12. https://doi.org/10.1177/1758835920971416 PMID: 33403013

21. Parekh V,Jacobs MA. Radiomics: a new application from established techniques. Expert Rev Precis Med Drug Dev. 2016; 1(2): 207–226. https://doi.org/10.1080/23808993.2016.1164013 PMID: 28042608

22. Gillies RJ, Kinahan PE,Hedvig Hricak. radiomics: Images Are More than Pictures, They Are Data. Radiology. 2016; 278(2): 563–577. https://doi.org/10.1148/radiol.2015151169 PMID: 26579733

23. Scheckenbach K, Colter L,Wagenmann M. Radiomics in Head and Neck Cancer: Extracting Valuable Information from Data beyond Recognition. ORL J Otorhinolaryngol Relat Spec. 2017; 79(1–2): 65–71. https://doi.org/10.1159/000455704 PMID: 28231582

24. Scheckenbach K, Colter L,Wagenmann M. The Potential of Radiomic-Based Phenotyping in Precision Medicine. JAMA Oncology. 2016; 2(12): 65–71. https://doi.org/10.1001/jamaoncol.2016.2631 PMID: 27541161

25. Kha QH, Ho QT,Le NQK. Identifying SNARE Proteins Using an Alignment-Free Method Based on Multiscan Convolutional Neural Network and PSSM Profiles. J Chem Inf Model. 2022; 62(19): 4820–4826. https://doi.org/10.1021/acs.jcim.2c01034 PMID: 36166351

26. Le NQK, Ho QT, Nguyen VN,Chang JS. BERT-Promoter: An improved sequence-based predictor of DNA promoter using BERT pre-trained model and SHAP feature selection. Comput Biol Chem. 2022; 99: 107732. https://doi.org/10.1016/j.compbiolchem.2022.107732 PMID: 35863177

27. Liu Tianyao, Zhao Zihan, Feng Baofu, Wang Xin, Li Tianhang, Xie Shangxun, et al. Robotic-assisted laparoscopic tumor enucleation is a feasible technique for renal hilar tumors: A retrospective study. J Surg Oncol. 2021; 124(1): 1–8. https://doi.org/10.1002/jso.26479 PMID: 33836093

28. Zhang Lu-Lu, Xu Fei, Song Di, Huang Meng-Yao, Huang Yong-Shi, Deng Qi-Ling, et al. Development of a Nomogram Model for Treatment of Nonmetastatic Nasopharyngeal Carcinoma. JAMA Network Open. 2020; 3(12): 1–14. https://doi.org/10.1001/jamanetworkopen.2020.29882 PMID: 33306119

29. Huang Jian-Feng, Sun Ren-Juan, Jiang Wen-Jun, Wu Ping, Zhang Li, Xu Mei-Qin, et al. Systematic nutrition management for locally advanced nasopharyngeal carcinoma patients undergoing radiotherapy. OncoTargets and Therapy. 2019; 2019(12): 8379–8386. https://doi.org/10.2147/OTT.S213789 PMID: 31632085

30. Wu Q, Liao W, Huang J, Zhang P, Zhang N,Li Q. Cost-effectiveness analysis of gemcitabine plus cisplatin versus docetaxel, cisplatin and fluorouracil for induction chemotherapy of locoregionally advanced nasopharyngeal carcinoma. Oral Oncol. 2020; 103: 1–7. https://doi.org/10.1016/j.oraloncology.2020.104588 PMID: 32070923

31. Chan ATC, Hui EP, Ngan RKC, Tung SY, Cheng ACK, Ng WT, et al. Analysis of Plasma Epstein-Barr Virus DNA in Nasopharyngeal Cancer After Chemoradiation to Identify High-Risk Patients for Adjuvant Chemotherapy: A Randomized Controlled Trial. J Clin Oncol. 2018; 2018(10): 1–10. https://doi.org/10.1200/JCO.2018.77.7847 PMID: 29989858

32. Hui EP, Li WF, Ma BB, Lam WKJ, Chan KCA, Mo F, et al. Integrating postradiotherapy plasma Epstein-Barr virus DNA and TNM stage for risk stratification of nasopharyngeal carcinoma to adjuvant therapy. Ann Oncol. 2020; 31(6): 769–779. https://doi.org/10.1016/j.annonc.2020.03.289 PMID: 32217076

33. Shen H, Yin J, Niu R, Lian Y, Huang Y, Tu C, et al. MRI-based radiomics to compare the survival benefit of induction chemotherapy plus concurrent chemoradiotherapy versus concurrent chemoradiotherapy plus adjuvant chemotherapy in locoregionally advanced nasopharyngeal carcinoma: A multicenter study. Radiother Oncol. 2022; 171: 107–113. https://doi.org/10.1016/j.radonc.2022.04.017 PMID: 35461950

34. Gao Y, Mao Y, Lu S, Tan L, Li G, Chen J, et al. Magnetic resonance imaging-based radiogenomics analysis for predicting prognosis and gene expression profile in advanced nasopharyngeal carcinoma. Head Neck. 2021; 43(12): 3730–3742. https://doi.org/10.1002/hed.26867 PMID: 34516714

35. Zhang L, Zhou H, Gu D, Tian J, Zhang B, Dong D, et al. Radiomic Nomogram: Pretreatment Evaluation of Local Recurrence in Nasopharyngeal Carcinoma based on MR Imaging. Journal of Cancer. 2019; 10(18): 4217–4225. https://doi.org/10.7150/jca.33345 PMID: 31413740

36. Bao D, Zhao Y, Liu Z, Zhong H, Geng Y, Lin M, et al. Prognostic and predictive value of radiomics features at MRI in nasopharyngeal carcinoma. Discov Oncol. 2021; 12(1): 63. https://doi.org/10.1007/s12672-021-00460-3 PMID: 34993528

37. Zhong L, Fang X-L, Dong D, Peng H,Fang M-J. A deep learning MR-based radiomic nomogram may predict survival for nasopharyngeal carcinoma patients with stage T3N1M0. Radiotherapy and Oncology. 2020; 8140(20): 1–25. https://doi.org/10.1016/j.radonc.2020.06.050 PMID: 32634460

38. Wu S, Li H, Dong A, Tian L, Ruan G, Liu L, et al. Differences in Radiomics Signatures Between Patients with Early and Advanced T-Stage Nasopharyngeal Carcinoma Facilitate Prognostication. J Magn Reson Imaging. 2021; 54(3): 854–865. https://doi.org/10.1002/jmri.27633 PMID: 33830573

39. Zhu C, Huang H, Liu X, Chen H, Jiang H, Liao C, et al. A Clinical-Radiomics Nomogram Based on Computed Tomography for Predicting Risk of Local Recurrence After Radiotherapy in Nasopharyngeal Carcinoma. Front Oncol. 2021; 11: 1–10. https://doi.org/10.3389/fonc.2021.637687 PMID: 33816279

40. Castellano G, Bonilha L, Li LM,Cendes F. Texture analysis of medical images. Clin Radiol. 2004; 59 (12): 1061–1069. https://doi.org/10.1016/j.crad.2004.07.008 PMID: 15556588

41. Chen BY, Xie H, Li Y, Jiang XH, Xiong L, Tang XF, et al. MRI-Based Radiomics Features to Predict Treatment Response to Neoadjuvant Chemotherapy in Locally Advanced Rectal Cancer: A Single Center, Prospective Study. Front Oncol. 2022; 12: 1–14. https://doi.org/10.3389/fonc.2022.801743 PMID: 35646677

42. Ye S, Han Y, Pan X, Niu K, Liao Y,Meng X. Association of CT-Based Delta Radiomics Biomarker With Progression-Free Survival in Patients With Colorectal Liver Metastases Undergo Chemotherapy. Front Oncol. 2022; 12: 1–10. https://doi.org/10.3389/fonc.2022.843991 PMID: 35692757

43. Fan M, Li H, Wang S, Zheng B, Zhang J,Li L. Radiomic analysis reveals DCE-MRI features for prediction of molecular subtypes of breast cancer. PLoS One. 2017; 12(2): 1–15. https://doi.org/10.1371/journal.pone.0171683 PMID: 28166261

44. Li S, Deng YQ, Zhu ZL, Hua HL,Tao ZZ. A Comprehensive Review on Radiomics and Deep Learning for Nasopharyngeal Carcinoma Imaging. Diagnostics (Basel). 2021; 11(9): 1–32. https://doi.org/10.3390/diagnostics11091523 PMID: 34573865

45. Zhang B, He X, Ouyang F, Gu D, Dong Y, Zhang L, et al. Radiomic machine-learning classifiers for prognostic biomarkers of advanced nasopharyngeal carcinoma. Cancer Lett. 2017; 403: 21–27. https://doi.org/10.1016/j.canlet.2017.06.004 PMID: 28610955

46. Gao A, Yang H, Wang Y, Zhao G, Wang C, Wang H, et al. Radiomics for the Prediction of Epilepsy in Patients With Frontal Glioma. Front Oncol. 2021; 11: 1–9. https://doi.org/10.3389/fonc.2021.725926 PMID: 34881174

47. Li H, Zhu M, Jian L, Bi F, Zhang X, Fang C, et al. Radiomic Score as a Potential Imaging Biomarker for Predicting Survival in Patients With Cervical Cancer. Front Oncol. 2021; 11: 1–9. https://doi.org/10.3389/fonc.2021.706043 PMID: 34485139

48. Zhuo EH, Zhang WJ, Li HJ, Zhang GY, Jing BZ, Zhou J, et al. Radiomics on multi-modalities MR sequences can subtype patients with non-metastatic nasopharyngeal carcinoma (NPC) into distinct survival subgroups. Eur Radiol. 2019; 29(10): 5590–5599. https://doi.org/10.1007/s00330-019-06075-1 PMID: 30874880

49. Feng Q, Liang J, Wang L, Niu J, Ge X, Pang P, et al. Radiomics Analysis and Correlation With Metabolic Parameters in Nasopharyngeal Carcinoma Based on PET/MR Imaging. Front Oncol. 2020; 10: 1–10. https://doi.org/10.3389/fonc.2020.01619 PMID: 33014815

50. Zhang B, Ouyang F, Gu D, Mo X, Huang W,Zhang S. Advanced nasopharyngeal carcinoma: pre-treatment prediction of progression based on multi-parametric MRI radiomics. Oncotarget. 2017; 8(42): 72457–72465. https://doi.org/10.18632/oncotarget.19799 eCollection 2017 Sep 22 PMID: 29069802

51. Jiang F, Jin T, Feng XL, Jin QF,Chen XZ. Long-term outcomes and failure patterns of patients with nasopharyngeal carcinoma staged by magnetic resonance imaging in intensity-modulated radiotherapy era: The Zhejiang Cancer Hospital's experience. J Cancer Res Ther. 2015; 11 Suppl 2: 179–184. https://doi.org/10.4103/0973-1482.168181 PMID: 26506872

52. Su L, Lin Q, Li R, Hua Y, Zhang H, Song X, et al. Prognostic value of nutritional impairment on treatment-related toxicity and survival in patients with nasopharyngeal carcinoma taking normal nutrition before radiotherapy. Head & Neck. 2020; 42(12): 3580–3589. https://doi.org/10.1002/hed.26426 PMID: 32851765

53. Shen DS, Yan C, Chen KH, Li L, Qu S,Zhu XD. A Nomogram Based on Circulating CD4(+) T Lymphocytes and Lactate Dehydrogenase to Predict Distant Metastasis in Patients with Nasopharyngeal Carcinoma. J Inflamm Res. 2021; 14: 6707–6718. https://doi.org/10.2147/JIR.S341897 PMID: 34916820

54. Guo R, Tang LL, Mao YP, Du XJ, Chen L, Zhang ZC, et al. Proposed modifications and incorporation of plasma Epstein-Barr virus DNA improve the TNM staging system for Epstein-Barr virus-related nasopharyngeal carcinoma. Cancer. 2019; 125(1): 79–89. https://doi.org/10.1002/cncr.31741 PMID: 30351466

55. Du YY, Luo DH, Sun XS, Tang LQ, Mai HQ, Chen QY, et al. Combining pretreatment plasma Epstein-Barr virus DNA level and cervical node necrosis improves prognostic stratification in patients with

nasopharyngeal carcinoma: A cohort study. Cancer Medicine. 2019; 8(16): 6841–6852. https://doi.org/10.1002/cam4.2481 PMID: 31513364

56. Chen Y-P, Liu X, Zhou Q, Yang K-Y, Jin F, Zhu X-D, et al. Metronomic capecitabine as adjuvant therapy in locoregionally advanced nasopharyngeal carcinoma: a multicentre, open-label, parallel-group, randomised, controlled, phase 3 trial. The Lancet. 2021; 398(10297): 303–313. https://doi.org/10.1016/S0140-6736(21)01123-5 PMID: 34111416

57. Peng H, Dong D, Fang MJ, Li L, Tang LL, Chen L, et al. Prognostic Value of Deep Learning PET/CT-Based Radiomics: Potential Role for Future Individual Induction Chemotherapy in Advanced Nasopharyngeal Carcinoma. Clin Cancer Res. 2019; 25(14): 4271–4279. https://doi.org/10.1158/1078-0432.CCR-18-3065 PMID: 30975664

58. Yongfeng P, Chuner J, Lei W, Fengqin Y, Zhimin Y, Zhenfu F, et al. The Usefulness of Pretreatment MR-Based Radiomics on Early Response of Neoadjuvant Chemotherapy in Patients With Locally Advanced Nasopharyngeal Carcinoma. Oncol Res. 2021; 28(6): 605–613. https://doi.org/10.3727/096504020X16022401878096 PMID: 33523792

59. Dong D, Zhang F, Zhong LZ, Fang MJ, Huang CL, Yao JJ, et al. Development and validation of a novel MR imaging predictor of response to induction chemotherapy in locoregionally advanced nasopharyngeal cancer: a randomized controlled trial substudy (NCT01245959). BMC Med. 2019; 17(1): 190. https://doi.org/10.1186/s12916-019-1422-6 PMID: 31640711

60. Keek S, Sanduleanu S, Wesseling F, de Roest R, van den Brekel M, van der Heijden M, et al. Computed tomography-derived radiomic signature of head and neck squamous cell carcinoma (peri)tumoral tissue for the prediction of locoregional recurrence and distant metastasis after concurrent chemo-radiotherapy. PLoS One. 2020; 15(5): e0232639. https://doi.org/10.1371/journal.pone.0232639 PMID: 32442178

61. Spadarella G, Calareso G, Garanzini E, Ugga L, Cuocolo A,Cuocolo R. MRI based radiomics in nasopharyngeal cancer: Systematic review and perspectives using radiomic quality score (RQS) assessment. Eur J Radiol. 2021; 140: 1–8. https://doi.org/10.1016/j.ejrad.2021.109744 PMID: 33962253

62. Zhang L, Ye Z, Ruan L,Jiang M. Pretreatment MRI-Derived Radiomics May Evaluate the Response of Different Induction Chemotherapy Regimens in Locally advanced Nasopharyngeal Carcinoma. Academic Radiology. 2020; 27(12): 1655–1664. https://doi.org/10.1016/j.acra.2020.09.002 PMID: 33004261